Modification of spontaneous emission in Bragg onion resonators

Wei Liang, Yanyi Huang and Amnon Yariv

Department of Applied Physics, MS 128-95, California Institute of Technology, Pasadena, CA 91125
liangwei@its.caltech.edu, yanyi@stanford.edu, ayariv@its.caltech.edu

Yong Xu

Department of Electrical and Computer Engineering (0111), Virginia Polytechnic Institute and State University, VA 24061
yong@vt.edu

Shawn-Yu Lin

Department of Physics, Applied Physics and Astronomy, Ressenlear Polytechnic Institute, Troy, New York, NY.
sylin@rpi.edu

Abstract: We formulated an analytical model and analyzed the modification of spontaneous emission in Bragg onion resonators. We consider both the case of a single light emitter and a uniformly distributed ensemble of light emitters within the resonator. We obtain an expression for the average radiation rate of the light emitters ensemble and discuss the modification of the average radiation rate as a function of cavity parameters such as the core radius, the number of Bragg cladding layers, the index contrast of the Bragg cladding, and the refractive index of surrounding medium. We also consider the possibility of non-exponential decay of the light emitter ensemble due to the strong dependence of spontaneous emission on the location and polarization of individual light emitter. We conclude that Bragg onion resonators can both enhance and inhibit spontaneous emission by several orders of magnitude. This property can have significant impact in the field of cavity quantum electrodynamics (QED).

OCIS codes: (230.5750) Resonators; (230.1480) Bragg reflectors; (270.5580) Quantum electrodynamics.

References and links

1. J. M. Gerard, D. Barrier,J. Y. Marzin,R. Kuszelewicz,L. Manin,E. Costard,V. ThierryMieg and T. Rivera, "Quantum boxes as active probes for photonic microstructures: The pillar microcavity case,"Appl. Phys. Lett. **69**, 449 (1996).
2. J. M. Gerard, and B. Gayral, "Strong Purcell effect for InAs quantum boxes in three-dimensional solid-state microcavities," J. Lightwave Technol. **17**, 2089 (1999).
3. B. Gayral, J. M. Gerard,A. Lemaitre,C. Dupuis,L. Manin and J. L. Pelouard, "High-Q wet-etched GaAs microdisks containing InAs quantum boxes,"Appl. Phys. Lett. **75**, 1908 (1999).
4. D. K. Armani, T. J. Kippenberg,S. M. Spillane and K. J. Vahala, "Ultra-high-Q toroid microcavity on a chip," Nature **421**, 925 (2003).
5. K. Srinivasan, P. E. Barclay,O. Painter,J. X. Chen,A. Y. Cho and C. Gmachl, "Experimental demonstration of a high quality factor photonic crystal microcavity," Appl. Phys. Lett. **83**, 1915 (2003).
6. K. J. Vahala, "Optical microcavities," Nature **424**, 839 (2003).
7. Y. Yamamoto, S. Machida and G. Bjork, "Microcavity Semiconductor-Laser with Enhanced Spontaneous Emission," Phys. Rev. A **44**, 657 (1991).
8. M. H. Macdougal, P. D. Dapkus,V. Pudikov,H. M. Zhao and G. M. Yang, "Ultralow Threshold Current Vertical-Cavity Surface-Emitting Lasers with Alas Oxide-Gaas Distributed Bragg Reflectors," IEEE Photon. Technol. Lett. **7**, 229 (1995).

#71220 - $15.00 USD Received 25 May 2006; revised 19 July 2006; accepted 20 July 2006

9. V. Sandoghdar, F. Treussart,J. Hare,V. LefevreSeguin,J. M. Raimond and S. Haroche, "Very low threshold whispering-gallery-mode microsphere laser," Phys. Rev. A. **54**, R1777 (1996).
10. D. L. Huffaker, L. A. Graham,H. Deng and D. G. Deppe, "Sub-40 mu A continuous-wave lasing in an oxidized vertical-cavity surface-emitting laser with dielectric mirrors," IEEE Photon. Technol. Lett. **8**, 974 (1996).
11. P. Michler, A. Kiraz,C. Becher,W. V. Schoenfeld,P. M. Petroff,L. D. Zhang,E. Hu and A. Imamoglu, "A quantum dot single-photon turnstile device," Science **290**, 2282 (2000).
12. J. M. Gerard, B. Sermage,B. Gayral,B. Legrand,E. Costard and V. Thierry-Mieg, "Enhanced spontaneous emission by quantum boxes in a monolithic optical microcavity," Phys. Rev. Lett. **81**, 1110 (1998).
13. M. Pelton, C. Santori,J. Vuckovic,B. Y. Zhang,G. S. Solomon,J. Plant and Y. Yamamoto, "Efficient source of single photons: A single quantum dot in a micropost microcavity," Phys. Rev. Lett**. 89** (2002).
14. Y. Xu, W. Liang,A. Yariv,J. G. Fleming and S. Y. Lin, "High-quality-factor Bragg onion resonators with omnidirectional reflector cladding," Opt. Lett. **28**, 2144 (2003).
15. Y. Xu, W. Liang,A. Yariv,J. G. Fleming and S. Y. Lin, "Modal analysis of Bragg onion resonators," Opt. Lett. **29**, 424 (2004).
16. K. G. Sullivan and D. G. Hall, "Radiation in Spherically Symmetrical Structures .2. Enhancement and Inhibition of Dipole Radiation in a Spherical Bragg Cavity," Phys. Rev. A. **50**, 2708 (1994).
17. R. R. Chance, A. Prock and R. Silbey, "Molecular fluorescence and energy transfer near interfaces," Adv. Chem. Phys. **37**, 1 (1978).
18. H. Chew, "Radiation and Lifetimes of Atoms inside Dielectric Particles," Phys. Rev. A. **38**, 3410 (1988).
19. W. Lukosz and R. E. Kunz, "Light-Emission by Magnetic and Electric Dipoles Close to a Plane Interface .1. Total Radiated Power," J. Opt. Soc. Am. **67**, 1607 (1977).
20. W. K. H. Panofsky and M. Phillips, Classical *electricity and Magnetism*, (Addison-Weskley, MA, 1956).
21. H. Chew, "Transition Rates of Atoms near Spherical Surfaces," J. Chem. Phys. **87**, 1355 (1987).
22. M. P. vanExter, G. Nienhuis and J. P. Woerdman, "Two simple expressions for the spontaneous emission factor beta," Phys. Rev. A. **54**, 3553 (1996).
23. E. Yablonovitch, "Inhibited Spontaneous Emission in Solid-State Physics and Electronics," Phys. Rev. Lett. **58**, 2059 (1987).
24. J. Vuckovic, M. Pelton,A. Scherer and Y. Yamamoto, "Optimization of three-dimensional micropost microcavities for cavity quantum electrodynamics," Phys. Rev. A. **66** (2002).
25. M. Bayer, T. L. Reinecke,F. Weidner,A. Larionov,A. McDonald and A. Forchel, "Inhibition and enhancement of the spontaneous emission of quantum dots in structured microresonators," Phys. Rev. Lett. **86**, 3168 (2001).
26. P. Das, and H. Metiu, "Enhancement of Molecular Fluorescence and Photochemistry by Small Metal Particles," J. Phys. Chem. **89**, 4680 (1985).
27. W. C. Chew, Waves and Fields in inhomogeneous Media (Van Nostrand Reinhold, New York, 1990).
28. Jackson, *Classical Electrodynamics* (John Wiley & Sons, Inc., New York, 1999).

1. Introduction

Optical microcavities, especially those that combine a large quality (*Q*) factor and a small modal volume *V*, have received much attention in recent years [1-6]. Such optical cavities can significantly enhance the electromagnetic density of states (DOS) and produce a large vacuum field fluctuation. As a result, it is possible to increase the interaction between the light emitter and the high Q cavity mode, which can be characterized by the Purcell factor Q/V, by several orders of magnitude. The enhanced interaction between the light emitting material and the high Q cavity mode can lead to many interesting effects in the field of cavity quantum electrodynamics, and plays a critical role in important applications such as “thresholdless” lasers [7-10] and single photon devices [11-13].

The high Q optical confinement in a microcavity is typically achieved through either total internal reflection or by utilizing a mixture of total internal reflection and Bragg reflection. For example, in silica microspheres, confinement through total internal reflection can create whispering-gallery modes with quality factors as high as 10^9. However, to satisfy the condition of total internal reflection, the sizes of such cavities are typically limited to tens of microns or greater. A large cavity size of such order of magnitude can create two significant drawbacks: it reduces the coupling strength between the light emitter and the high Q optical mode, and makes it more difficult to achieve a truly single mode operation (due to the small frequency spacing between adjacent high Q modes). On the other hand, optical microcavities based on Bragg reflections can have much smaller sizes of the order of λ/n, which is ideal for applications demanding strong interactions between the light emitter and the vacuum field. An example of Bragg-confined optical cavities is a semiconductor micropillar [1], where one uses Bragg

#71220 - $15.00 USD Received 25 May 2006; revised 19 July 2006; accepted 20 July 2006

reflection to confine light in one dimension (1D) and total internal reflection to confine light in the other two dimensions. Another case of Bragg cavity is a defect structure embedded in a two-dimensional (2D) photonic crystal [5], where one employs 2D photonic band gap (PBG) effect to achieve Bragg confinement in the two dimensional plane of photonic crystal, and use total internal reflection to confine photons in the third dimension.

From the brief discussion above, it is clear that most of the high Q optical microcavities in the literature involve some degrees of total internal reflection confinement, which creates a significant drawback: By involving total internal reflection, it is always possible for the light emitter within the cavity to interact with the radiation modes that extend into the free space. The emission rate into these undesired radiation modes can be lumped together, and represented as the background radiation rate Γ_{bg}. The emission rate into the desired high Q mode can be labeled as Γ_{mode}. For efficient single photon source, we need to design a cavity structure to achieve $\Gamma_{mode} >> \Gamma_{bg}$.

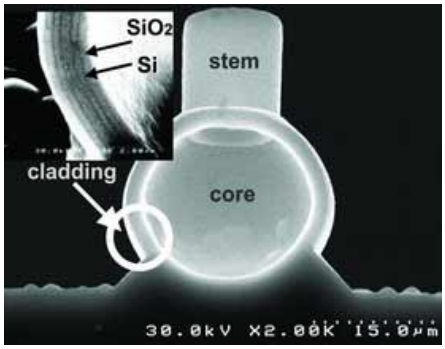

Fig. 1. SEM image of a sliced Bragg onion resonator.

In this paper, we focus on a new class of optical microcavities, namely Bragg onion resonators, that have been developed by the authors and reported in Ref. [14, 15]. The most interesting feature of the onion resonators is the unique possibility of approaching true three dimensional confinement in such microcavities. A scanning electron micrograph (SEM) image of these optical cavities is shown in Fig. 1. As can be seen from the SEM figure, the onion resonator is composed of a spherical hollow core bound by concentric layers of alternating dielectric materials (silicon and SiO_2 in this example). With the large index contrast of silicon and SiO_2, the spherical Bragg stack forms an omnidirectional mirror that approaches the behavior of a perfect metal and reflects nearly all incident light, regardless of the incident angle and polarization. Under this condition and assuming a completely spherical onion resonator (without the stem section in Fig. 1, the vacuum fields within and without the onion cavity are completely separated. If we place a light emitter within the hollow onion core, the light emitter can only couple to two classes of onion resonator modes: either the *core modes* that are mostly confined within the hollow core, or the *cladding modes* that concentrate their energy within the dielectric cladding layers of the onion resonators. Consequently, the coupling between the light emitter and the core mode are significantly stronger than the light-emitter and cladding mode coupling. With these considerations, we can conclude that if the frequency of the light emitter coincides with resonant frequencies of the core modes, we can expect a significant enhancement of spontaneous emission rate. On the other hand, if the light emitter frequency does not coincide with any of the core modes, the onion resonator can significantly inhibit the spontaneous emission process of the light emitting material.

From the discussion above, it is clear that in terms of spontaneous emission engineering, there is a major distinction between the conventional optical microcavities and Bragg onion resonators. In conventional cavities, the reliance on total internal reflection invariably leads to a

#71220 - $15.00 USD Received 25 May 2006; revised 19 July 2006; accepted 20 July 2006

significant background radiation rate Γ_{bg}, which corresponds to the radiation into the free space traveling mode. On the other hand, with the presence of the omnidirectional cladding layers, the fully spherically symmetric Bragg onion resonators can almost completely suppress the coupling into the free space radiation mode. Consequently, we can achieve both spontaneous emission enhancement and spontaneous emission inhibition of up to several orders of magnitude. In other words, we can use onion resonators to obtain a significantly increased Γ_{mode} (the radiation rate into the desired high Q optical mode), and at the same time dramatically reduce the background radiation rate Γ_{bg}. This unique property should make the Bragg onion resonator a near ideal candidate for single photon devices.

To analyze spontaneous emission modifications induced by the onion resonator, we begin with a simplified model that ignores the presence of onion stem section in Fig. 1 and analyze onion resonators with full spherical symmetry. This assumption allows us to develop an analytical model for the calculation of spontaneous emission rate and establish a basic understanding of the spontaneous emission process within the onion core. Furthermore, we notice that the main effect of the onion stem section is in allowing the interaction of free space vacuum field and the light emitter through the stem section. Consequently, the presence of the stem section will lead to an additional increase of background emission rate that can be estimated as $\Gamma_{free}(\Delta\Omega/4\pi)$, where Γ_{free} is the free space spontaneous emission rate, and $\Delta\Omega$ is the solid angle spanned by the onion stem. From this estimate, it is also clear that we can significantly reduce this additional background emission rate to a very low level by decreasing the onion stem diameter to the level of 1 μm [14].

In the literature, some studies have been published on the modification of spontaneous emission in spherical dielectric microspheres and spherical Bragg cavities [16]. However, the previous studies only consider a Bragg sphere with a continuously varying cladding and assume that the radiation source is located at the center of the sphere. In this paper, we adopt a transfer matrix approach to analyze the discrete cladding layers with a very large index contrast. We further extend the discussion to an ensemble average of dipoles uniformly distributed within the cavity core, which may provide a more realistic picture of what can be achieved in experiments. We also focus our analysis on Bragg onion resonators that closely resemble the actually fabricated structures, which provides us a physical understanding and is highly relevant for the experimental demonstration of spontaneous emission modification in Bragg onion resonators.

The paper is organized as follows: In section II, we begin with a classical model of a damped dipole oscillator driven by electromagnetic waves reflected by the microcavity [16,17]. We combine such a classical picture with the transfer matrix method developed in Ref. [14], which allows us to calculate the radiation rate of a dipole source arbitrarily located within the Bragg onion resonator core. In section III we present a detailed numerical study of the modified spontaneous emission process in Bragg onion resonators with various parameters. We conclude this paper in section IV.

2. Spontaneous emission of a single dipole in a Bragg onion resonator

The modified spontaneous emission of a light emitter in an optical microcavity can be analyzed using a classical model. In this model, which was developed in Ref. [16], the light emitter is described as an oscillating electric dipole that interacts with its own reflected field [16,18,19]. The modified spontaneous emission rate is given by the decay rate of a dipole oscillator governed by the following equation:

$$\ddot{p} + \omega_0^2 p = (q^2/m)E_R(t) - b_0\dot{p} \tag{1}$$

where p is the electric dipole moment of the atomic transition, ω_0 is the intrinsic dipole oscillation frequency in the absence of all damping, and b_0 is the spontaneous emission rate of a light emitter in the bulk material. The extra term $(q^2/m)E_R(t)$ in Eq. (1) accounts for the modification of spontaneous emission rate within the microcavity. More precisely, $E_R(t)$ is the component of the reflected field (due to the microcavity) that is located at the position of the

#71220 - $15.00 USD Received 25 May 2006; revised 19 July 2006; accepted 20 July 2006

dipole source and is parallel to the dipole moment. The two parameters q and m respectively describe the effective charge and the effective mass of the dipole oscillator. The exact values of q and m are not significant, since they only appear in the final expression of the modified spontaneous emission rate in the form of:

$$m/q^2 = n_0\omega_0^2/(6\pi\varepsilon_0 b_0 c_0^{\,3}) \tag{2}$$

where $n_0=(\varepsilon/\varepsilon_0)^{1/2}$ is the refractive index of the bulk core material, ε_0 and c_0 are respectively the permittivity and the speed of light in free space. The relation Eq. (2) is derived using the classical radiation dipole model. For a more detailed explanation, the reader can consult Ref. [20].

In order to find the solution of Eq. (1), we assume that both the dipole moment p and the reflected field component $E_R(t)$ oscillate at the same modified complex frequency:

$$p = p_0 \exp\left[-(i\varpi + b/2)t\right] \tag{3a}$$

$$E_R(t) = E_0 \exp\left[-(i\varpi + b/2)t\right] \tag{3b}$$

where b corresponds to the modified spontaneous emission rate, ω is the modified emission frequency, p_0 and E_0 are respectively the amplitudes of the dipole moment and the reflected field component. By substituting Eqs. (2) and (3) into Eq. (1), we find that the normalized spontaneous emission rate and frequency shift in the presence of the micro-cavity are given by:

$$b/b_0 = 1 + \mathrm{Re}(E_0/E_S) \tag{4a}$$

$$(\omega-\omega_0)/b_0 = 1/2\cdot \mathrm{Im}(E_0/E_S) \tag{4b}$$

where we assume that both b and $\Delta\omega = \omega - \omega_0$ are much smaller than ω_0. The two terms E_S, and E_0 in Eq. (4) are respectively given by:

$$E_S = i\mu_0\omega_0^2 p_0 k/6\pi \tag{5a}$$

$$E_0 = \varepsilon^{-1}\lim_{\vec{r}\to\vec{r}_o}\left\{\hat{\vec{\alpha}}\cdot\left[D_R^{TE}(\vec{r}) + D_R^{TM}(\vec{r})\right]\right\} \tag{5b}$$

where $k = \sqrt{\varepsilon/\varepsilon_0}\,\omega_0/c_0$ is the wave vector, ε and μ_0 are respectively the permittivity and permeability of the bulk material. In the case of Bragg onion resonators, since the light emitters are confined within the onion core, ε and μ_0 also represent the permittivity and permeability of the core material. In Eq. (5b), $\hat{\vec{\alpha}}$ is the unit vector along the orientation of the light emitting dipole, and E_0 is defined after Eq. (3b). The two terms D_R^{TE} and D_R^{TM} correspond to, respectively, the transverse electric (TE) and transverse magnetic (TM) component of the reflected field, which can be obtained using dyadic Green's function. Due to the spherical symmetry of the onion resonator, we can separate D_R^{TE} and D_R^{TM} into multiple components using spherical harmonics expansion and characterize each component with a pair of angular quantum numbers l, and m. The detailed forms of D_R^{TE} and D_R^{TM} are given in Appendix A as Eq. (A4a)-(A4b). With some straightforward calculation and application of appropriate boundary conditions, we find the following expression for E_0:

$$\frac{E_0}{E_s} = 12\pi\sum_{l=1}^{\infty}\sum_{m=-l}^{l}\left[\frac{\rho_l^{TE}h_l^1(kr_{co})}{h_l^2(kr_{co}) - \rho_l^{TE}h_l^1(kr_{co})}\cdot\left|\hat{\vec{\alpha}}\cdot\vec{E}_{lm}^{TE}(\vec{r}_0)\right|^2 + \frac{\rho_l^{TM}h_l^1(kr_{co})}{h_l^2(kr_{co}) - \rho_l^{TM}h_l^1(kr_{co})}\cdot\left|\hat{\vec{\alpha}}\cdot\vec{E}_{lm}^{TM}(\vec{r}_0)\right|^2\right] \tag{6}$$

The detailed derivation of Eq. (6) is given in Appendix A. Here it suffices to mention that $j_l(kr)$ and $h_l(kr)$ are respectively the lth order spherical Bessel and Hankel function, whereas $\vec{E}_{lm}^{TM}$ and $\vec{E}_{lm}^{TE}$ are defined as:

#71220 - $15.00 USD Received 25 May 2006; revised 19 July 2006; accepted 20 July 2006

$$\vec{E}_{lm}^{TM} = \vec{\nabla} \times j_l(kr)\vec{X}_{lm} / k \tag{7a}$$

$$\vec{E}_{lm}^{TE} = j_l(kr)\hat{L}Y_{lm}(\theta,\varphi)/\sqrt{l(l+1)} = j_l(kr)\vec{X}_{lm} \tag{7b}$$

In Eq. (7), $\vec{X}_{lm} = \hat{L} \cdot Y_{lm}(\theta,\varphi)\Big/\sqrt{l(l+1)}$ is the spherical vector function. The only undefined quantities in Eq. (6) are the two parameters ρ_l^{TE} and ρ_l^{TM}, which are defined as the field amplitude reflection coefficients of the *l*th order TE and TM multipole modes at the interface between the onion core and the innermost cladding layer [16].The amplitude reflection coefficients ρ_l^{TE} and ρ_l^{TM} can be calculated using the transfer matrix method described in Ref. [14, 15] and the derivation is summarized as follows.

First, the field in each dielectric layer of the onion resonator can be expressed as a superposition of different (*l*,*m*) multipole orders. Due to the spherical symmetry of the structure, individual multipole fields with different *l* and *m* are independent of each other. For a given pair of angular quantum number *l* and *m*, the TE or TM components within the *n*th dielectric layer is:

$$\begin{bmatrix} \vec{H} \\ \vec{E} \end{bmatrix} = \begin{bmatrix} h_l^1(k_n r)\vec{X}_{l,m} & h_l^2(k_n r)\vec{X}_{l,m} \\ Z_n \cdot i/k_n \cdot \vec{\nabla} \times h_l^1(k_n r)\vec{X}_{l,m} & Z_n \cdot i/k_n \cdot \vec{\nabla} \times h_l^2(k_n r)\vec{X}_{l,m} \end{bmatrix} \cdot \begin{bmatrix} A_n \\ B_n \end{bmatrix} \quad \text{(TM)} \tag{8a}$$

$$\begin{bmatrix} \vec{E} \\ \vec{H} \end{bmatrix} = \begin{bmatrix} Z_n h_l^1(k_n r)\vec{X}_{l,m} & Z_n h_l^2(k_n r)\vec{X}_{l,m} \\ -i/k_n \cdot \vec{\nabla} \times h_l^1(k_n r)\vec{X}_{l,m} & -i/k_n \cdot \vec{\nabla} \times h_l^2(k_n r)\vec{X}_{l,m} \end{bmatrix} \cdot \begin{bmatrix} C_n \\ D_n \end{bmatrix} \quad \text{(TE)} \tag{8b}$$

where $Z_n=(\mu_0/\varepsilon_n)^{1/2}$ is the material impedance, and $k_n=(\varepsilon_n/\varepsilon_0)^{1/2}\omega_0/c_0$ is the wave vector within the *n*th layer. The four linear coefficients A_n, B_n, C_n and D_n, are constant within the *n*th layer. Since the spherical Hankel functions $h_l^1(kr_{co})$ and $h_l^2(kr_{co})$ represent, respectively, the outgoing and the incoming wave, the amplitude reflection coefficient ρ_l at the core-cladding interface in Eq. (7) is can be determined from Eq. (8) as [16]

$$\rho_l^{TM} = \frac{B_{co}h_l^2(kr_{co})}{A_{co}h_l^1(kr_{co})} \;\; \& \;\; \rho_l^{TE} = \frac{D_{co}h_l^2(kr_{co})}{C_{co}h_l^1(kr_{co})} \tag{9}$$

Employing the continuity condition of $E_\theta, E_\phi, H_\theta, H_\phi$ at the interface between two adjacent layers and the orthogonality of the spherical harmonics, we can relate the linear coefficients in the onion core (A_{co}, B_{co}, C_{co}, D_{co}) to those outside the onion resonator (A_{out}, B_{out}, C_{out}, D_{out}) through two by two matrices M_l^{TM} and M_l^{TE} [14]:

$$\begin{bmatrix} A_{co} \\ B_{co} \end{bmatrix} = M_l^{TM} \cdot \begin{bmatrix} A_{out} \\ B_{out} \end{bmatrix} \text{(TM mode)} \;\&\; \begin{bmatrix} C_{co} \\ D_{co} \end{bmatrix} = M_l^{TE} \cdot \begin{bmatrix} C_{out} \\ D_{out} \end{bmatrix} \text{(TE mode)} \tag{10}$$

Combining Eq. (10) with the boundary condition that there is no incoming wave outside the onion resonator, i.e. $B_{out}=0$ and $D_{out}=0$, we can express B_{co}/A_{co} and C_{co}/D_{co} as a function of the individual elements of the two-by-two matrices M_l^{TM} and M_l^{TE}:

$$\begin{aligned} B_{co}/A_{co} &= \left(M_l^{TM}\right)_{2,1} / \left(M_l^{TM}\right)_{1,1} \\ D_{co}/C_{co} &= \left(M_l^{TE}\right)_{2,1} / \left(M_l^{TE}\right)_{1,1} \end{aligned} \tag{11}$$

The subscripts of 1 or 2 in the equation above refer to the row and column indices of the matrix element. Substituting Eq. (11) into Eq. (9), we find:

#71220 - $15.00 USD Received 25 May 2006; revised 19 July 2006; accepted 20 July 2006

$$\rho_l^{TM} = \frac{\left(M_l^{TM}\right)_{2,1} h_l^2(kr_{co})}{\left(M_l^{TM}\right)_{1,1} h_l^1(kr_{co})} \quad \& \quad \rho_l^{TE} = \frac{\left(M_l^{TE}\right)_{2,1} h_l^2(kr_{co})}{\left(M_l^{TE}\right)_{1,1} h_l^1(kr_{co})} \tag{12}$$

Applying Eq. (6)-(7) and Eq. (12) to Eq. (4a)-(4b), the normalized modified spontaneous emission rate and the frequency shift take the form of

$$\frac{b}{b_0} = 1 + 12\pi \sum_{l=1}^{\infty} \sum_{m=-l}^{l} \mathrm{Re}\left(\frac{\left(M_l^{TM,TE}\right)_{2,1}}{\left(M_l^{TM,TE}\right)_{1,1} - \left(M_l^{TM,TE}\right)_{2,1}} \right) \cdot \left| \vec{\alpha} \cdot \vec{E}_{lm}^{TM,TE}(\vec{r}_0) \right|^2 \tag{13a}$$

$$\frac{\Delta\omega}{b_0} = 6\pi \sum_{l=1}^{\infty} \sum_{m=-l}^{l} \mathrm{Im}\left(\frac{\left(M_l^{TM,TE}\right)_{2,1}}{\left(M_l^{TM,TE}\right)_{1,1} - \left(M_l^{TM,TE}\right)_{2,1}} \right) \cdot \left| \vec{\alpha} \cdot \vec{E}_{lm}^{TM,TE}(\vec{r}_0) \right|^2 \tag{13b}$$

where the superscript *TM,TE* implies summation over both TM and TE modes.

In the literature, there is another classical approach that gives the modified spontaneous emission rate [17,19,21]. In this model, the decaying rate in the presence of the cavity normalized by the bulk emission rate is identical to the total radiation power of a classical dipole in the micro-cavity, P_{cav}, divided by the dipole radiation power in the bulk material, P_{bulk}. Using this approach, we demonstrate in Appendix B that the normalized modified spontaneous emission rate can also be expressed as

$$\frac{b}{b_0} = \frac{P_{cav}}{P_{bulk}} = 12\pi \sum_{l=1}^{\infty} \sum_{m=-l}^{l} \frac{1}{2} \left| \frac{1}{\left(M_l^{TM,TE}\right)_{1,1} - \left(M_l^{TM,TE}\right)_{2,1}} \right|^2 \left| \vec{\alpha} \cdot \vec{E}_{lm}^{TM,TE}(\vec{r}_0)^2 \right| \tag{14}$$

In deriving above equation I assumed the core and the outer space of the Bragg onion resonator are filled with the same material. In Appendix B, we prove that this formula is equivalent to the result given in Eq. (13a). The advantage of Eq. (14) compared to Eq. (13a) is that the contribution of each individual multipole component to the total spontaneous emission rate is explicitly given, which can be used to test the convergence of the calculated spontaneous emission rate.

3. Numerical results and analysis

In this section, we use the analytical algorithm described in the previous section to study the spontaneous emission modification in an onion resonator. We first calculate the spontaneous emission rate of a single dipole emitter arbitrarily located within the onion cavity core. Next, we extend the analysis to an ensemble of dipoles uniformly distributed within the cavity core and study the dependence of the average spontaneous emission rate on various cavity parameters. Finally we briefly consider the non-exponential decaying of the dipole ensemble due to their non-uniformly decaying behavior. In all calculations, we use parameters similar to the samples that have been successfully fabricated and reported in Ref. [15]. The core is assumed to be air unless specified otherwise. We mainly consider two types of onion resonators: One with cladding layers composed of silicon and SiO_2, the other one with cladding layer composed of SiO_2 and Si_3N_4. For the onion resonators considered in this paper, the silicon cladding layers have a refractive index of 3.5 and a thickness of 0.111 μm, whereas the refractive index and the thickness of the SiO_2 layers are respectively 1.5 and 0.258 μm. For the Si_3N_4 layers, the refractive index is 2.1 and the thickness is 0.185 μm. The parameters of the Bragg cladding pairs are chosen such that the bandgap center is located at 1.55 μm.

3.1 A single dipole emitter located at the center of the onion resonator

We first consider the simplest case of spontaneous emission modification in the onion resonator, in which a single dipole is positioned at the center of the onion resonator. In this case, the dipole can only couple to the TM_1 mode, since this is the only multipole component that

#71220 - $15.00 USD Received 25 May 2006; revised 19 July 2006; accepted 20 July 2006

provides a non-zero contribution to the summation in Eq. (13) [16]. The numerical results of the modified spontaneous emission rate and the frequency shift are plotted in Fig. 2(a)-(c). As expected, if the dipole emission frequency coincides with the frequency of the onion resonator modes, the spontaneous emission rate can be significantly enhanced, and the enhancement ratio increases with the addition of more Bragg cladding layers. On the other hand, if the dipole emission frequency does not coincide with any of the cavity modal frequencies, the spontaneous emission rate can be reduced by several orders of magnitude. In fact, with just six Bragg layers, we can achieve spontaneous emission enhancement of approximately 10^4 times in the on-resonance case and spontaneous emission inhibition of the order of 10^{-4} in the off-resonance case.

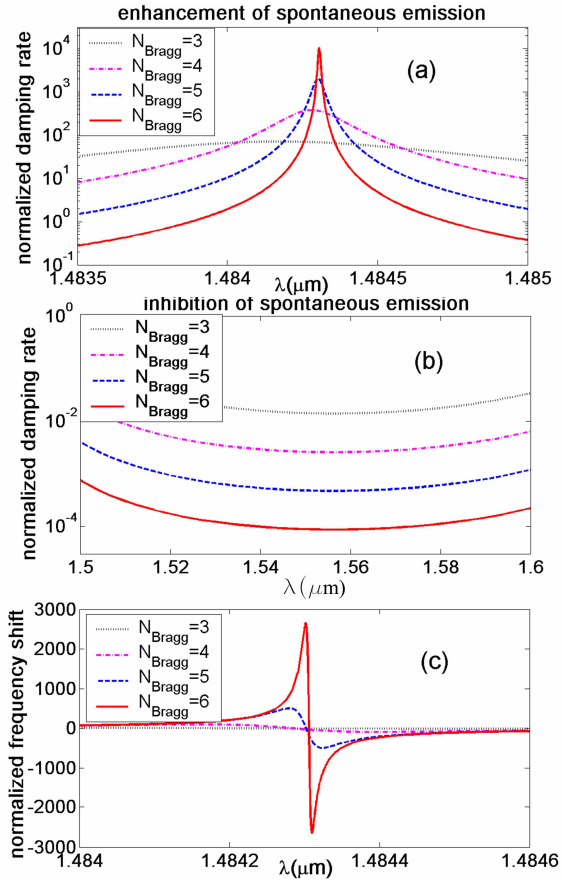

Fig. 2. (a). Enhancement of the spontaneous emission. (b). Inhibition of the spontaneous emission. (c). Spectral dependence of the normalized frequency shift. Here the dipole is fixed at the center of the Bragg onion sphere. The dotted, dash-dotted, dashed and solid lines correspond to a rising Bragg layer number of N_{Bragg} = 3, 4, 5 and 6.

3.2 Dependence of modified spontaneous emission rate on the dipole position

Here we consider the dependence of the spontaneous emission rate on the position of a single dipole emitter located within the onion core. Due to the spherical symmetry of the structure, we can always assume that the dipole is located on the $\hat{z}$ axis and its corresponding spherical coordinate is $\vec{r}_0 = (r, 0, 0)$. In this case, the spontaneous emission rate depends on both the displacement from the center of the onion resonator, r, and the orientation of the

#71220 - $15.00 USD Received 25 May 2006; revised 19 July 2006; accepted 20 July 2006

dipole oscillator $\hat{\vec{\alpha}}$. We can further decompose the dipole polarization $\hat{\vec{\alpha}}$ into a radial component and a transverse component and consider only two cases: the radial polarization case where $\hat{\vec{\alpha}}$ aligns along the radial direction; and the case of transverse polarization where $\hat{\vec{\alpha}}$ lies within the transverse plane. For these two different polarization cases, we respectively denote the corresponding spontaneous emission rate as $b^{\perp}$ (radial) and $b^{//}$ (transverse). Without a loss of generality, we can also assume that $\hat{\vec{\alpha}}$ is along the *x* axis in the case of transverse polarization. Substituting $\vec{r}_0 = (r, 0, 0)$ into Eq. (13a) we find:

$$\frac{b^{\perp}}{b_0} = 1 + 3\sum_{l=1}^{\infty} \mathrm{Re}\left(\frac{\left(M_l^{TM}\right)_{2,1}}{\left(M_l^{TM}\right)_{1,1} - \left(M_l^{TM}\right)_{2,1}} \right) \cdot l(l+1)(2l+1)\frac{j_l^2}{(kr)^2} \tag{15a}$$

$$\frac{b^{//}}{b_0} = 1 + \frac{3}{2}\sum_{l=1}^{\infty} (2l+1)\mathrm{Re}\left\{ \frac{\left(M_l^{TM}\right)_{2,1}}{\left(M_l^{TM}\right)_{1,1} - \left(M_l^{TM}\right)_{2,1}} \left[\frac{d(krj_l)}{kr \cdot d(kr)} \right]^2 + \frac{\left(M_l^{TE}\right)_{2,1}}{\left(M_l^{TE}\right)_{1,1} - \left(M_l^{TE}\right)_{2,1}} j_l^2 \right\} \tag{15b}$$

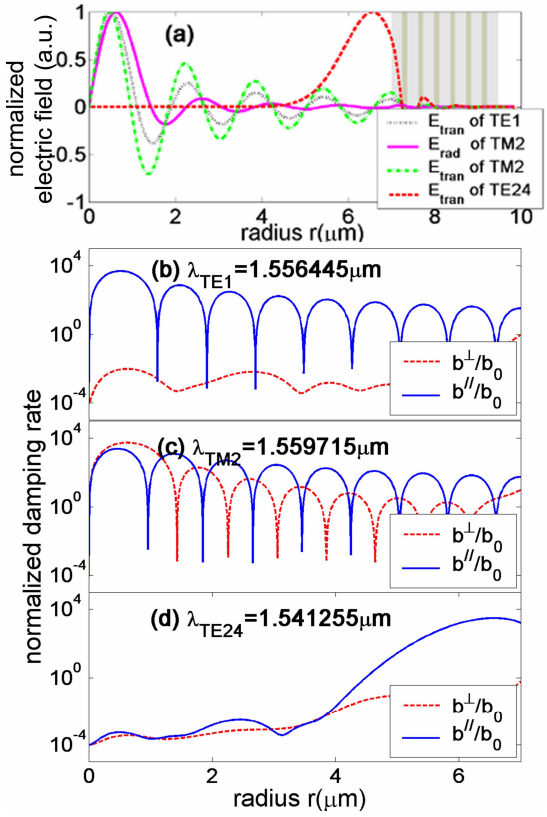

Fig. 3. (a). Radial dependence of the electric field of TE_1, TM_2 and TE_{24} eigenmodes. TE_1 and TE_{24} modes only have a transverse electric component while TM_2 mode has both the radial and the transverse electric components. (b)–(d). Radial dependence of the normalized radial damping rate $b^{\perp}/b_0$ (red dashed line) and transverse $b^{//}/b_0$ (blue solid line). Results in (b)–(d) are calculated at the wavelength λ =1.556445μm, 1.559715μm and 1.541255μm, which are the eigen-wavelength of TE_1, TM_2 and TE_{24} modes respectively. N_{Bragg} = 6 is used here.

#71220 - $15.00 USD
Received 25 May 2006; revised 19 July 2006; accepted 20 July 2006

In Fig. 3(b)-(d), we show the normalized spontaneous emission rates for the radial ($b^{\perp}/b_0$) and the transverse ($b^{//}/b_0$) polarization as a function of the dipole position. We first consider three different modes (TE_1, TM_2 and TE_{24} modes) and calculate the spontaneous emission rate at the three corresponding modal wavelengths (λ =1.556445μm, 1.559715μm and 1.541255μm). The radial dependence of the electric field of the TE_1, TM_2 and TE_{24} mode are also plotted In Fig. 3(a). As can be seen from Fig. 3(a)-(d), at the resonant wavelength of the onion cavity mode, the spatial dependence of the spontaneous emission rate of a single dipole emitter follows the electric field distribution of the corresponding resonant mode. Such behavior can be explained by the fact that in the "on-resonance" case, the spontaneous emission process is dominated by the radiation into the resonant high Q mode. The other interesting point is that at the resonance of a TE mode (see Fig. 3(b) and Fig. 3(d), the spontaneous emission of a dipole oscillating along the radial direction ($b^{\perp}/b_0$) is strongly inhibited, whereas that of a dipole oscillating along the tangential direction is significantly enhanced. This is due to the fact that the radial component of the electric field of TE modes is zero. Consequently the dipole polarized along the radial direction can only couple to the TM modes, which is off resonance at the given wavelength.

3.3 Radiation from a dipole ensemble within the onion resonator core

In experiments, it can be very challenging to place a single light emitter (such as an organic molecule or a gas phase atom) at a specific location within the onion resonator core. Instead, it's easier to fill the entire onion core with an ensemble of light emitters. By exciting the light emitters and measuring the temporal variation of the radiation power, we can experimentally extract the ensemble average of the modified spontaneous emission rate. In this case, both the spatial position and the orientation of the dipoles have a strong dependence on the external parameters such as the profile and polarization of the excitation field. For a quantitative estimate, we assume that the light emitting dipoles are uniformly distributed within the entire onion core with random polarizations (as in Ref [18]). Consequently, the spontaneous emission rate at a given position $\vec{r}$ averaged over all possible dipole orientation, i.e. $\langle b(\vec{r})/b_0 \rangle_{dir}$, is given by:

$$\langle b(\vec{r})/b_0 \rangle_{dir} = \int b(\vec{r},\Omega)/b_0 d\Omega/4\pi \tag{16}$$

where the angular integration is over all the possible polarization directions. By substituting Eq. (13a) into Eq. (16), we notice that for each multipole order *(l, m)*, the contribution to the average spontaneous emission rate involves the integration of $\left|\hat{\vec{\alpha}}\cdot\vec{E}_{lm}^{TM,TE}\right|^2$ over the angular distribution of the dipole source, which can be simplified as:

$$\int\left|\hat{\vec{\alpha}}\cdot\vec{E}_{lm}^{TM,TE}\right|^2 d\Omega/4\pi = \left(\left(\vec{E}_{lm}^{TM,TE}\right)_r^2 + \left(\vec{E}_{lm}^{TM,TE}\right)_\theta^2 + \left(\vec{E}_{lm}^{TM,TE}\right)_\varphi^2\right)/3 \tag{17}$$

where $\hat{\vec{\alpha}}$ is the unit vector representing the dipole orientation, and $\vec{E}_{lm}^{TM,TE}$ is the electric field defined in Eq. (7a)-(7b). Since the first term on the right hand side of Eq. (17) corresponds to the radial spontaneous emission rate and both the second and the third term correspond to the transverse spontaneous emission rate, we can simplify Eq. (16) as:

$$\langle b(\vec{r})/b_0 \rangle_{dir} = \left(b^{\perp}/b_0 + 2\cdot b^{//}/b_0\right)/3 \tag{18}$$

with $b^{\perp}/b_0$ and $b^{//}/b_0$ given in Eq. (15a) and Eq. (15b). Next we need to average $\langle b(\vec{r})/b_0 \rangle_{dir}$ over the spatial distribution of the dipole sources to have the ensemble-averaged spontaneous emission decaying rate $\langle b/b_0 \rangle_{vol}$, which is

#71220 - $15.00 USD Received 25 May 2006; revised 19 July 2006; accepted 20 July 2006

$$\left\langle b/b_0 \right\rangle_{vol} = \int_0^{r_{co}} \left\langle b(\vec{r})/b_0 \right\rangle_{dir} d^3\vec{r} \Big/ \left(\frac{4}{3}\pi {r_{co}}^3 \right) \tag{19}$$

where r_{co} is the radius of the onion resonator core. Substituting Eq. (15a)-(15b) and Eq. (18) into Eq. (19) and using the integral identity of the Bessel functions [18], we obtain

$$\left\langle b/b_0 \right\rangle_{vol} = 1 + \frac{3}{r_{co}^3} \sum_{l=1}^{\infty} (2l+1) \mathrm{Re}\left\{ \frac{\left(M_l^{TM}\right)_{2,1}}{\left(M_l^{TM}\right)_{1,1} - \left(M_l^{TM}\right)_{2,1}} P_l + \frac{\left(M_l^{TE}\right)_{2,1}}{\left(M_l^{TE}\right)_{1,1} - \left(M_l^{TE}\right)_{2,1}} Q_l \right\} \tag{20}$$

where P_l and Q_l are the integrals of the Bessel functions and take the form of

$$Q_l = \frac{1}{2}(kr_{co})^3 \left[{j_l}^2(kr_{co}) - j_{l+1}(kr_{co}) j_{l-1}(kr_{co}) \right] \quad \& \quad P_l = Q_{l-1} - l \cdot kr_{co} {j_l}^2(kr_{co}) \tag{21}$$

We can also calculate the average spontaneous emission rate by using the alternative expression for the spontaneous emission rate (Eq. (14)). Following the same procedure, we find that the average spontaneous emission rate can also be expressed as:

$$\left\langle b/b_0 \right\rangle_{vol} = \frac{3}{(kr_{co})^3} \sum_{l=1}^{\infty} \frac{(2l+1)}{2} \left[\left| \frac{1}{\left(M_l^{TM}\right)_{1,1} - \left(M_l^{TM}\right)_{2,1}} \right|^2 P_l + \left| \frac{1}{\left(M_l^{TE}\right)_{1,1} - \left(M_l^{TE}\right)_{2,1}} \right|^2 Q_l \right] \tag{22}$$

Since according to Eq. (22) the cavity modified spontaneous emission rate has contributions from all multipole orders, it is necessary to investigate the convergence of the summation in the equation. We first classify the onion resonator modes with various multipole order l into two groups[1]: the core modes (which concentrate within the cavity core and are confined by the Bragg reflection), and the cladding modes (which are mainly confined in the cladding layers through total internal reflection (TIR)). The core modes typically have smaller angular quantum number l that satisfies $l \le n_{co} 2\pi \cdot r_{co} / \lambda$, where n_{co} is the refractive index of the onion resonator core. Examples of core modes are shown in Fig. 3(a). The cladding modes generally have angular quantum number l greater than $n_{co} 2\pi \cdot r_{co} / \lambda$. Examples of cladding modes are shown in Fig. 4.

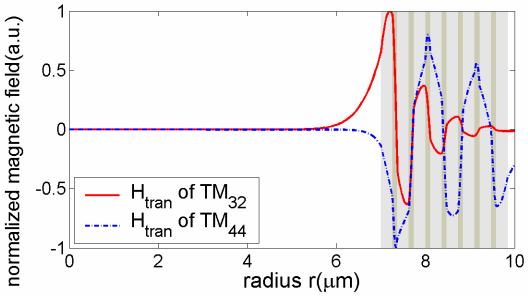

Fig. 4. The radial dependence of the magnetic field of the cladding modes. The fields of both modes are evanescent in the core. The field of TM_{32} mode decays quickly in the cladding due to the Bragg reflection. While the field of TM_{44} mode is propagating in the cladding layer and is confined by TIR at the outer surface. Here we use $r_{co} = 7\mu m$ and $N_{Bragg} = 7$.

In Fig. 5, we use three different onion structures to illustrate the relative strength of spontaneous emission into different mutlipole order l. We use Eq. (22) and choose the wavelength at 1.543 μm, which is an off-resonance case for all three different onion cavities. The parameters of the onion resonators are given in the figure and the figure caption. As can

#71220 - $15.00 USD
Received 25 May 2006; revised 19 July 2006; accepted 20 July 2006

be seen from the figure, most of the contributions to the ensemble-averaged total spontaneous emission rate come from the core modes (l <30 for $r_{co} = 7\mu m$) and some cladding modes (45>l>30 for $r_{co} = 7\mu m$)). The contributions from the cladding modes with very large angular quantum number l decrease very fast, which ensures the convergence of the summation in Eq. (20) and (22).

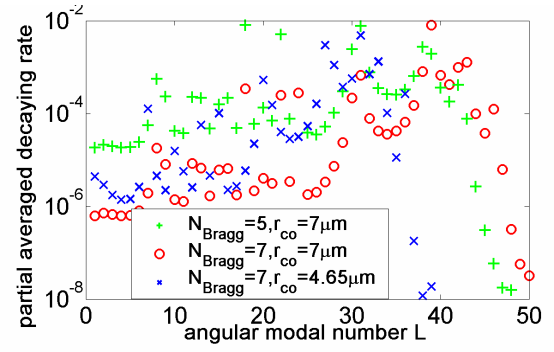

Fig. 5. The partial averaged spontaneous emission rate as a function of the modal number L (i.e. the lth term in Eq. (22)).

Fig. 5 also has several other interesting features. First we notice that the core modes with l less than 10 does not contribute significantly to the cavity modified spontaneous emission rate, which is due to the fact that the light emitter frequency does not coincide with any of the core modes. It is also clear that among the cladding modes, those with a relatively smaller angular quantum number l have a much stronger coupling to the light emitter within the onion core. This can be explained by the observation that the cladding modes with smaller l penetrate deeper into the onion core, as shown in Fig. 4.

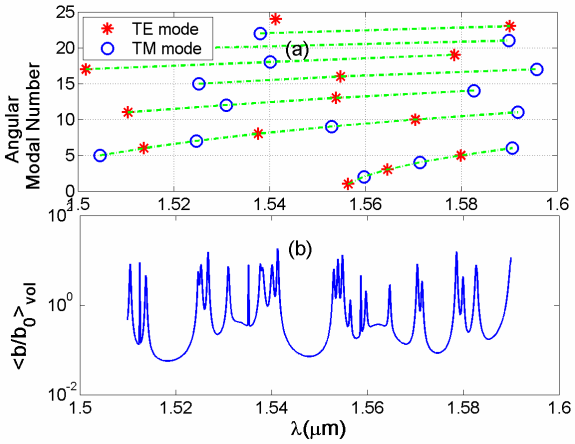

Fig. 6. (a) Spectrum of the onion resonator eigenmodes with modal number $l \le 24$. (b). Spectral dependence of the ensemble averaged damping rate. $r_{co} = 7\mu m$ and $N_{Bragg} = 4$ are used in the calculation.

In Fig. 6(b) we plot the spectral dependence of the average spontaneous emission rate for an onion resonator with four pairs of cladding layers. The frequencies of the onion resonator

#71220 - $15.00 USD
Received 25 May 2006; revised 19 July 2006; accepted 20 July 2006

modes are calculated using the transfer matrix method [14] and shown in Fig. 6(a). It is evident that the peak positions in spontaneous emission rate spectrum (Fig. 6(b)) match the wavelengths of the onion resonator modes shown in Fig. 6(a). Furthermore, we notice that with only four pairs of cladding layers, we can already achieve an average inhibition of the order of 0.05~0.1 in the off resonance and an enhancement of the order of 10 if the light emitter frequency coincides with that of the onion resonator modes.

For the on-resonance cases, if we ignore the linewidth of the light emitting material (as in our calculations), the enhancement of the spontaneous emission rate at the resonant frequency of a dominant cavity mode can be estimated as [15, 22]

$$\beta = \left\langle b / b_0 \right\rangle_{vol} = Q_{cav} \lambda^3 / \left(4\pi^2 V_{cav}^{eff}\right) \tag{23}$$

where λ is the optical wavelength, V_{cav}^{eff} is the effective modal volume and Q_{cav} is the quality factor of the cavity mode. Since the quality factor of the core modes increases exponentially as a function of the cladding layer number [14], we expect that the resonance enhancement of spontaneous emission rate also increases exponentially with N_{clad}. As an example, we calculate the peak enhancement ratio $\left\langle b / b_0 \right\rangle_{vol}$ at the resonant wavelength of the TE_1, TM_2 and TE_{24} modes as a function of the cladding pair number N_{Bragg}. The results, which are given in Fig. 7, clearly demonstrate an excellent exponential dependence.

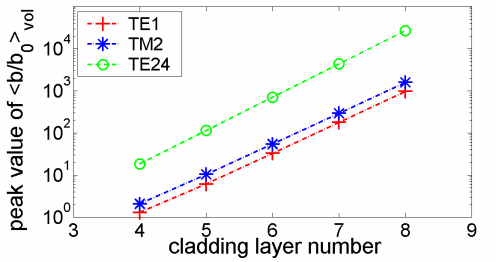

Fig. 7. Enhancement of the ensemble averaged spontaneous emission decaying rate as a function of the cladding layer number. The "plus", "star" and "circle" are values of the peaks in Fig. 6 corresponding to TE_1, TM_2 and TE_{24} resonance modes respectively.

3.4 Spontaneous emission inhibition in Bragg onion resonators

A unique feature of the onion resonators is the possibility of significant spontaneous emission inhibition, which is important for many quantum optics applications [6,7,23-25]**.** If the onion resonator has cladding layers with a very large index contrast and a sufficiently large core radius, the onion cladding layer can be regarded as an omnidirectional reflector, which behaves as perfect metal and can effectively isolate the vacuum field within the onion resonator from the free space vacuum field. In this case, the light emitter within the onion core can no longer couple to the free space vacuum field, which lead to significant spontaneous emission inhibition in the onion cavity, as we have observed in previous analytical results. However, for onion resonators with a small number of cladding pairs, or those with relatively low-index contrast cladding layers, or smaller core radius, the aforementioned simple analysis may no longer apply. In this section, we analyze the spontaneous emission inhibition of dipole ensembles in onion resonators with different parameters such as cladding pair number N_{Bragg}, cladding index contrast, core radius, and the refractive index of the core material. We focus primarily on cases where we may no longer approximate the onion cladding layers as an omnidirectional mirror any more. We demonstrate that even for such "non-ideal" onion resonators, we can still achieve spontaneous emission suppression for at least two orders of magnitude.

#71220 - $15.00 USD Received 25 May 2006; revised 19 July 2006; accepted 20 July 2006

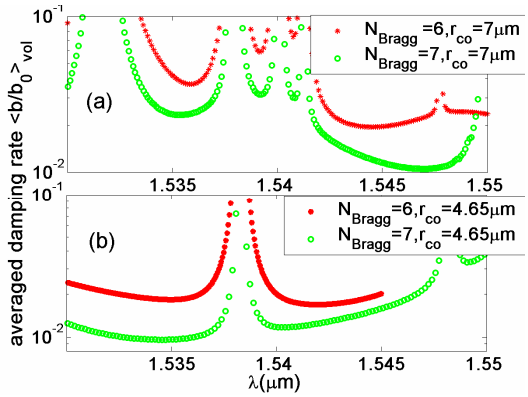

Fig. 8. Suppression of the damping rate for different core radii of 7μm and 4.65 μm respectively. In both (a) and (b), the green circles and the red stars correspond to Bragg layer number N_{Bragg} = 6 and 7 respectively.

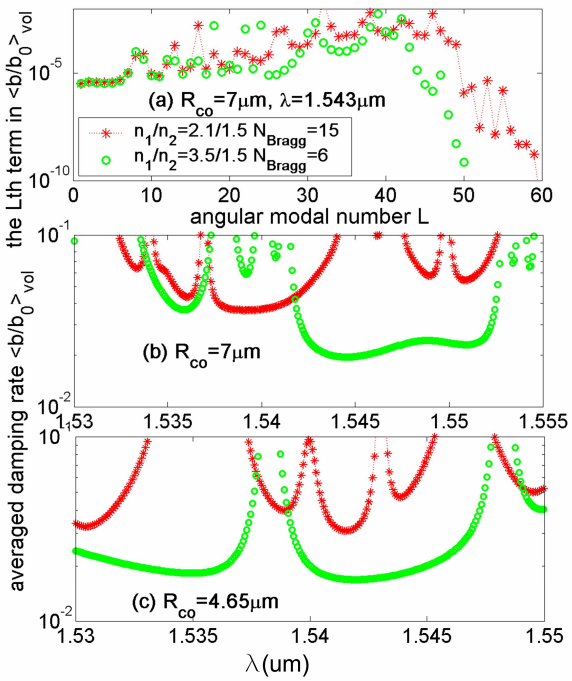

Fig. 9. (a) The partial averaged damping rate as a function of the modal number *l* (the *l*th term in Eq. (22)). (b) and (c). Averaged damping rate for different cladding layer index contrast. We use core radius of 7μm in (a) and (b), and 4.65μm in (c). The data is calculated at $\lambda = 1.543\mu m$ in (a). In all figures, the red "asterisk" is for $n_1/n_2 = 2.1/1.5$ and N_{Brag},= 15, the green "circle" is for $n_1/n_2 = 3.5/1.5$ and N_{Bragg} = 6.

We first study the dependence of the spontaneous emission inhibition on the cladding pair number N_{Bragg}, assuming the core radius to be 7 μm. It is instructive to first consider the results in Fig. 5. Comparing the two cases (one with N_{Bragg} = 5 and the other with N_{Bragg} = 7), we find that the additional cladding layers significantly reduce the spontaneous emission rate into multipole components with small angular quantum number (l<30). The spontaneous emission rate into larger multipole components (38< l <44), however, remains approximately

#71220 - $15.00 USD Received 25 May 2006; revised 19 July 2006; accepted 20 July 2006

the same even as N_{Bragg} increases. This is to be expected since the larger multipole components account for contributions from the cladding modes. In Fig. 8, we show the spectra of total average spontaneous emission rate in onion resonators with two different core radii. The results clearly show that we can achieve spontaneous emission inhibition up to two orders of magnitude with seven pairs of cladding layers, and the radius of the onion core does not have a significant impact on the degrees of spontaneous emission inhibition.

The cladding layers of onion resonators can be constructed from other dielectric materials besides Si and SiO2. Using a fabrication technique similar to those discussed in Ref. [14], we can realize onion resonators with SiO2 and Si3N4 as cladding layer materials. Since both SiO2 and Si3N4 are transparent for visible light, the onion resonators with SiO2/Si3N4 cladding layers are ideal for applications in the visible range. However, due to a smaller index contrast, the SiO2/Si3N4 cladding layers no longer form omnidirectional reflectors. Therefore, it is of interests to investigate the inhibition of spontaneous emission in onion resonators with SiO2/Si3N4 cladding. The parameters of the SiO2/Si3N4 layers in our calculations are given at the beginning of section 3.

For comparison among various onion resonators with different cladding materials, we choose to compare those with similar quality factors, since the cavity quality factor is the one parameter that can effectively describe the separation between the high Q cavity mode and the free space radiation mode, which is of the utmost importance in our analysis. With this requirement in mind, we will compare SiO_2/Si_3N_4 onion resonators with 15 cladding pairs with SiO_2/Si onion resonators of 6 cladding pairs. The quality factors of the TE_1 mode in these two onion resonators are respectively 1.9613×10^5 and 1.8759×10^5. In Fig. 9(a), we show the averaged spontaneous emission rate into various multipole order l in SiO_2/Si_3N_4 and SiO_2/Si onion resonators. We notice that for the SiO_2/Si_3N_4 and the SiO_2/Si onion resonators, the spontaneous emission rate into a given multipole order l are very similar in magnitude if the multipole order l is relatively small. On the other hand, for larger multipole orders, the partial spontaneous emission rate of the SiO_2/Si_3N_4 onion resonator is generally larger than that of the SiO_2/Si onion resonators. Such behavior can be attributed to the fact that the SiO_2/Si cladding layers can provide optical confinement equally well for both larger and smaller multipole orders (due to their large index contrast), whereas the SiO_2/Si_3N_4 cladding layers are less effective in providing confinement for radiation fields with larger multipole orders. In Fig. 9(b) and Fig. 9(c), we show the total average spontaneous emission rate in a SiO_2/Si_3N_4 onion resonator and a corresponding SiO_2/Si onion resonator. The results demonstrate that for two Bragg onion resonators with similar quality factors, the one with SiO_2/Si cladding layers can achieve better spontaneous emission inhibition as compared to the resonator with SiO_2/Si_3N_4 cladding layers. However, it should be noted that the degree of spontaneous emission inhibition in a SiO_2/Si_3N_4 onion resonator is only marginally less than that of a comparable SiO_2/Si onion resonator, which is approximately a factor of two.

In order to experimentally investigate spontaneous emission modification in a Bragg onion resonator, one particular attractive approach is to immerse the entire onion structure into water based solution doped with light emitting materials. In Fig. 10, we compare the spontaneous emission inhibition in an air-core onion resonator with an onion resonator filled with water-based solution. With a larger refractive index (n_{co} = 1.33), the wave vector in a water-filled onion resonator is smaller compared to that in an air core onion resonator, which means an onion resonator with a water-filled core can support higher order multipole modes. Therefore, the light emitter within the solution filled onion cavity can couple to more mutlipole components, which is clearly shown in Fig. 10(a). As a result, we expect that the inhibition of spontaneous emission should be less pronounced in the water core onion resonator as compared to the air core onion resonator. In Fig. 10(b) and (10c), we show the total average spontaneous emission rate in a water core onion resonator and the corresponding air core resonator. As expected, the off resonance spontaneous emission rate in a water core onion resonator is similar or slightly larger than that in an air core resonator. However, our calculations also demonstrate

#71220 - $15.00 USD Received 25 May 2006; revised 19 July 2006; accepted 20 July 2006

that it is possible to achieve a two orders of magnitude reduction in the spontaneous emission rate in a solution-filled onion resonator.

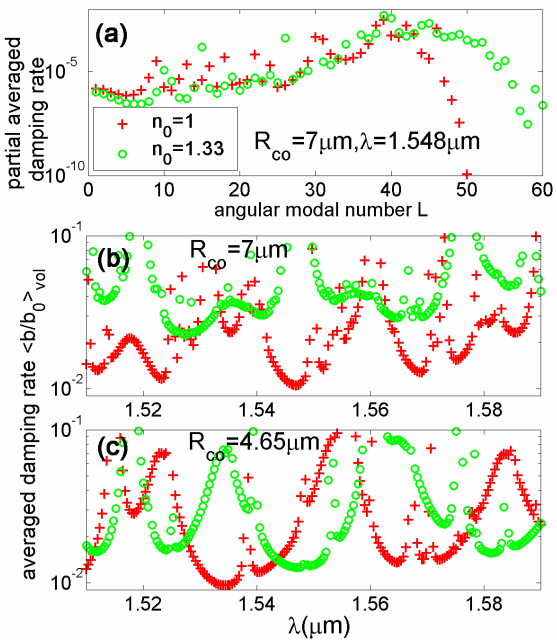

Fig. 10. (a) The partial averaged damping rate as a function of the modal number *l* (the *l*th term in Eq. (22)). (b) and (c). The averaged damping rate for the Bragg onion resonator immersed in different media. We assume the core area and surrounding area are filled with the light emitting media whose index is n_0. We use core radius of 7μm in (a) and (b), and 4.65μm in (c). The data is calculated at $\lambda = 1.548\mu m$ in (a)-(c). In all figures, we use N_{Bragg} = 7, n_0 =1 for the "asterisk" and n_0 =1.33 for the "circle".

3.5 Non-exponential averaged decaying

In the above analysis of onion resonators, we assume that the average spontaneous emission rate provides an adequate description of the spontaneous emission process in the microcavity. However, due to the sharp variation of spontaneous emission rate as a function of both the position and polarization of the light emitter, we expect that the spontaneous emission from the dipole ensemble within the onion core can be non-exponential, and an average spontaneous emission rate does not contain the complete information on the cavity modified spontaneous emission process. In this section, we provide a few examples that illustrate a more complicated picture for the spontaneous emission in the onion resonator.

In order to simplify our analysis, we assume that all of the light emitters within the onion core are excited at the time *t* = 0. Subsequently at a later time *t*, the total number of light emitters at the excited state is

$$N(t) = \iint \exp\left(-b(\vec{r},\Omega)\cdot t\right)\cdot n(\vec{r},\Omega) d^3\vec{r}\cdot d\Omega / 4\pi \qquad (24)$$

where $n(\vec{r},\Omega)$ describes the initial distribution of the light emitters at the excited state as a function of the dipole position $\vec{r}$ and polarization $\Omega = (\theta,\varphi)$. To further simplify calculations, we assume the initial distribution function $n(\vec{r},\Omega)$ to be a constant number n_0

#71220 - $15.00 USD Received 25 May 2006; revised 19 July 2006; accepted 20 July 2006

and consider the local spontaneous emission rate to be independent of the dipole polarization. In reality, the spontaneous emission rate of an individual dipole source may have a strong dependence on the dipole polarization (as shown in Fig. 3). However, the assumption of a polarization independent local spontaneous emission rate greatly simplifies the integration in Eq. (24), and also allows a qualitatively analysis of the non-exponential spontaneous decay in the onion resonator. With these considerations, Eq. 24 is simplified as:

$$N(t) = n_0 \iint \exp\left(-\left\langle b(\vec{r})/b_0 \right\rangle_{dir} \cdot t\right) d^3\vec{r} \tag{25}$$

where $\left\langle b(\vec{r})/b_0 \right\rangle_{dir}$ is the local spontaneous emission rate averaged over all the possible dipole orientation and is given by Eq. (18). The optical radiation power due to the dipole ensemble in the onion core can be obtained from Eq. (25):

$$P(t) = \hbar\upsilon \cdot dN(t)/dt = \hbar\upsilon n_0 \iint \exp\left(-\left\langle b(\vec{r})/b_0 \right\rangle_{dir} \cdot t\right) \left\langle b(\vec{r})/b_0 \right\rangle_{dir} d^3\vec{r} \tag{26}$$

where $\hbar\upsilon$ is the energy of a single photon. From Eq. (26), we can define a time dependent average damping rate as

$$b(t) = 1/P(t) \cdot \left(dP(t)/dt\right) \tag{27}$$

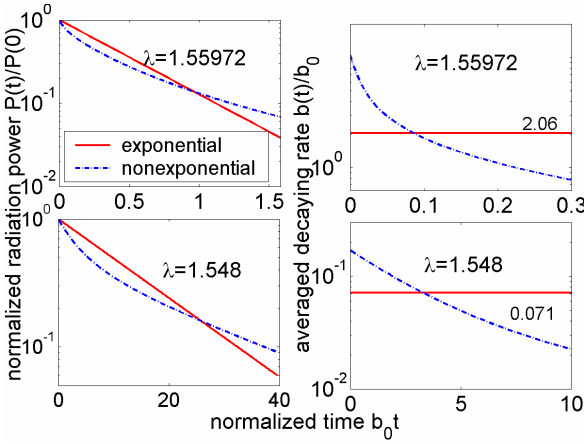

Fig. 11. Normalized radiation power (the left column) and the derived averaged decaying rate $b(t)$ (the right column) as a function of time. The red solid line stands for the exponential decaying, the blue dashed line stands for the non-exponential decaying. The exponential decaying rate is calculated with Eq. (22). We use parameters r_{co} = 7 μm, N_{Bragg} = 4 in the calculation and choose two wavelengths: 1.55972μm (eigenwavelength of TM2 mode) and 1.548μm (off resonance).

For an onion resonator with a core radius of 7 μm and four pairs of SiO_2/Si cladding pairs, we analyze the time dependent spontaneous emission at λ = 1.55972μm, which correspond to the resonant wavelength of the TM_2 mode, and λ=1.548μm, which is off cavity resonance. In Fig. 11, we plot the temporal variation of the spontaneous radiation power and the time dependent spontaneous emission rate. From Fig. 11, we notice that initially, the total radiation power calculated from Eq. (26) decays faster than the results obtained assuming exponential decay. On the other hand, at later time the rate of non-exponential decay becomes smaller than the average spontaneous emission rate obtained assuming exponential decay. Since the spontaneous emission from the light emitter ensemble contains both fast-decaying

#71220 - $15.00 USD Received 25 May 2006; revised 19 July 2006; accepted 20 July 2006

and slow-decaying dipoles, it is reasonable to expect that the total radiation from the dipole ensemble begins with contributions from fast-decaying light emitters followed by slow-decaying light emitters, as shown in Fig. 11. From the results shown in Fig. 11, we can also conclude that the average spontaneous emission rate as defined in Eq. (22) provides a reasonably good description of the decay of the dipole ensemble within the onion resonator, even though the time dependent spontaneous emission rate changes after the initial excitation.

4. Discussion

In above analysis, we assume the structure is a perfect onion sphere and haven't addressed the influence on the spontaneous emission of the open stem in the real sample shown in Fig. 1. We estimated in Ref [14] that the presence of the stem has very little impact on the quality factor of the core modes, thus it won't have significant influence on the resonance enhancement ratio. In practice, the observation of Purcell effect in a high Q cavity is limited by the large spectral width of commonly used emitters (~20nm at 300K for rare-earth atoms [12]). To date, quantum dots are used extensively to study the Purcell effect in semiconductors because of their narrow spectral lineshape [12,25]. In the case of radiation suppression, we pointed out in Ref [14] the contribution of the "stem" leakage to the radiation rate can be roughly estimated from the fraction of the solid angle spanned by the "stem", or $b_{stem}/b_0 = (r_{stem}/2r_{co})^2$. The practical value for the stem radius and the core radius are 1μm and 7μm, thus we obtain b_{stem}/b_0 ~ 0.5%. In our analysis (e.g., Fig. 9), a suppressed of ~1% can be achieved with N_{Bragg} = 7. Thus we expect that the suppression ratio can be limited by the presence of the stem only for very large N_{Bragg} > 8.

5. Conclusion

In this paper, we utilize two different approaches to calculate the spontaneous emission of a dipole inside the core of a Bragg Onion spherical resonator. Using the parameters of the realized structure, we calculate the detuning of the modified spontaneous emission of a dipole located at the center and the profile of the damping rate as a function of the dipole position. To account for the real case, we further calculate the average damping rate for an ensemble of excited emitters inside the core. Dependence of the ensemble-averaged damping rate on different parameters is also discussed. An enhancement ratio of $10^2 \sim 10^3$ upon resonance and a suppression ratio of $\sim 10^{-2}$ off resonance can be achieved with 7 Bragg cladding layers. Finally, the assumption that the averaged radiation decays exponentially is examined. The analysis presented in this paper should provide a quantitative foundation for future experimental investigation of onion resoantors.

Appendix

A. Derivation of the reflected electric field

To calculate the field reflected by the cladding layers, we start with the result given in Ref [16] and summarize it as follows. For an oscillating dipole located at position $\vec{r}_0$ in the Bragg onion core and polarized along direction $\hat{\vec{\alpha}}$, the source field is governed by the vector wave equation (assuming $\exp(-i\omega_0 t)$ harmonic time dependence)

$$\vec{\nabla}\times\vec{\nabla}\times\vec{D}_s(\vec{r}) - \omega_0^2\mu_0\varepsilon\vec{D}_s(\vec{r}) = i\mu_0\omega_0\varepsilon\vec{J}(\vec{r}) \qquad \text{(A1)}$$

Where ω_0 is the angular frequency, μ_0 and ε are the constant permeability and permittivity of the core material, $\vec{J} = -i\omega_0 p_0 \delta(\vec{r}-\vec{r}_0)\hat{\vec{\alpha}}$ is the current density, and p_0 is the amplitude of the dipole moment. Employing the dyadic Green's function method [26], the transverse magnetic (TM) component and transverse electric (TE) component of the source field satisfy

#71220 - $15.00 USD Received 25 May 2006; revised 19 July 2006; accepted 20 July 2006

$$\left[\vec{r}\cdot\vec{D}_s(\vec{r})\right]^{TM} = iJ_0/\omega_0\cdot\vec{r}\cdot\vec{\nabla}_0\times\vec{\nabla}_0\times\vec{r}_0 g(\vec{r},\vec{r}_0),\quad \vec{r}\neq\vec{r}_0 \tag{A2a}$$

$$\left[\vec{r}\cdot\vec{B}_s(\vec{r})\right]^{TE} = \mu_0 J_0\hat{\vec{\alpha}}\cdot\vec{\nabla}_0\times\vec{r}_0 g(\vec{r},\vec{r}_0),\qquad \vec{r}\neq\vec{r}_0 \tag{A2b}$$

where $J_0 = -i\omega_0 p_0$ is the current amplitude, $g(\vec{r},\vec{r}_0) = \exp\left(ik\left|\vec{r}-\vec{r}_0\right|\right)/4\pi\left|\vec{r}-\vec{r}_0\right|$ is the three-dimensional scalar Green's function. The subscript "$_0$" in the gradient operator $\vec{\nabla}_0$ means the operator is acting on the source variable $\vec{r}_0$. $g(\vec{r},\vec{r}_0)$ can be expanded in terms of spherical waves such that

$$g(\vec{r},\vec{r}_0) = ik\sum_{l=0}^{\infty}\sum_{m=-l}^{l} j_l(kr_<)h_l^1(kr_>)Y_{lm}(\theta,\varphi)Y_{lm}^*(\theta_0,\varphi_0) \tag{A3}$$

where $j(kr_<)$ and $h_l^1(kr_>)$ are respectively the spherical Bessel function and the spherical Hankel function of the first kind, $Y_{lm}(\theta,\varphi)$ is the spherical harmonics function, $r_>$ ($r_<$) is the greater (lesser) of r and r_0. The reflected field is coming from the source field reflected by the cladding and should have similar forms to the source field. We can thus express the reflected fields according to Eq. (A2a)-(A3) as

$$\vec{D}_R^{TM}(\vec{r}) = -i\vec{\nabla}\times\left[O_S^{TM}(\vec{r}_0)\sum_{l=0}^{\infty}\sum_{m=-l}^{l}\frac{1}{l(l+1)}2(A_{lm})^{TM}\, j_l(kr)\hat{L}Y_{lm}(\theta,\varphi)\right] \tag{A4a}$$

$$\vec{D}_R^{TE}(\vec{r}) = \varepsilon\omega_0 O_S^{TE}(\vec{r}_0)\sum_{l=0}^{\infty}\sum_{m=-l}^{l}\frac{1}{l(l+1)}2(A_{lm})^{TE}\, j_l(kr)\hat{L}Y_{lm}(\theta,\varphi) \tag{A4b}$$

where $(A_{lm})^{TE,TM}$ are constant amplitudes decided by boundary condition, $\hat{L} = \vec{r}\times\vec{\nabla}/i$ is the angular momentum operator, $O_S^{TM}(\vec{r}_0)$ and $O_S^{TE}(\vec{r}_0)$ are operators acting on the source variable, which can be expressed as

$$O_S^{TM}(\vec{r}_0) = -kJ_0/\omega_0\cdot\hat{\vec{\alpha}}\cdot\vec{\nabla}_0\times\vec{\nabla}_0\times\vec{r}_0 \tag{A5a}$$

$$O_S^{TE}(\vec{r}_0) = i\mu_0 kJ_0\hat{\vec{\alpha}}\cdot\vec{\nabla}_0\times\vec{r}_0 \tag{A5b}$$

In Eq. (A4a)-(A4b) we only employ the spherical Bessel function of the first kind, $j_l(kr)$, because the reflected field must be nonsingular at the center $r = 0$. The total field in the core is the sum of the source field and the reflected field and must satisfy the boundary conditions: at the core-cladding interface, the sum of the inward-traveling radial waves is equal to the sum of the product of the outward-traveling radial waves and the field amplitude reflection coefficient. Employing the boundary condition we obtain the constant amplitudes

$$(A_{lm})^{TE,TM} = \frac{\rho_l^{TE,TM} h_l^1(kr_{co}) j_l(kr_0) Y_{lm}^*(\theta_0,\varphi_0)}{h_l^2(kr_{co}) - \rho_l^{TE,TM} h_l^1(kr_{co})} \tag{A6}$$

where ρ_l is the field amplitude reflection coefficient of the l th order multipole mode at the core-cladding interface, r_{co} is the radius of the core. Substituting Eq. (A6) into Eq. (A4a)-(A4b), and applying the result to Eq. (5b), the reflected electric field component along the dipole moment orientation at the source position normalized by parameter E_S (Eq. (5a)) is

$$\frac{E_R}{E_S} = 12\pi\sum_{l=1}^{\infty}\sum_{m=-l}^{l}\left[\frac{\rho_l^{TE} h_l^1(kr_{co})}{h_l^2(kr_{co}) - \rho_l^{TE} h_l^1(kr_{co})}\cdot\left|\hat{\vec{\alpha}}\cdot\vec{E}_{lm}^{TE}(\vec{r}_0)\right|^2 + \frac{\rho_l^{TM} h_l^1(kr_{co})}{h_l^2(kr_{co}) - \rho_l^{TM} h_l^1(kr_{co})}\cdot\left|\hat{\vec{\alpha}}\cdot\vec{E}_{lm}^{TM}(\vec{r}_0)\right|^2\right] \tag{A7}$$

#71220 - $15.00 USD
Received 25 May 2006; revised 19 July 2006; accepted 20 July 2006

where the vectors $\vec{E}_{lm}^{TM}$ and $\vec{E}_{lm}^{TE}$ are defined as

$$\vec{E}_{lm}^{TM} = \vec{\nabla} \times j_l(kr)\vec{X}_{lm} / k \tag{A8a}$$

$$\vec{E}_{lm}^{TE} = j_l(kr)\hat{L}Y_{lm}(\theta,\varphi) = j_l(kr)\vec{X}_{lm} / \sqrt{l(l+1)} \tag{A8b}$$

where $\vec{X}_{lm} = \hat{L} \cdot Y_{lm}(\theta,\varphi) / \sqrt{l(l+1)}$ is the spherical vector function [27]. In the summation in Eq. (A7), the term with $l = 0$ is dropped because $\vec{X}_{00}(\theta,\varphi) \equiv 0$.

B. Direct evaluation of the modified decaying rate by calculating the radiation power

In this section, we derive the modified spontaneous emission rate (Eq. (13a)) using another classical approach [17,19,21,26]. In this model, the decaying rate in the presence of the cavity normalized by the bulk emission rate is identical to the total radiation power of a classical dipole in the micro-cavity, P_{cav}, divided by the dipole radiation power in the bulk material, P_{bulk}. For an oscillating dipole located at $\vec{r}_0$, the radiative electric field at $r > r_0$ in the core can be expanded in terms of the multipole modes [28]

$$\vec{E}_{dip} = Z_{co} \sum_{l,m} \left[i/k_{co} \cdot a_E(l,m)\vec{\nabla} \times h_l^1(k_{co}r)\vec{X}_{lm} + a_M(l,m)h_l^1(k_{co}r)\vec{X}_{lm} \right] \tag{B1}$$

where

$$a_E(l,m) = -i \cdot k_{co}^2 / \sqrt{l(l+1)} \cdot \int Y_{lm}^* \left\{ c\rho \frac{d}{dr}[rj_l(k_{co}r)] + ik_{co}(\vec{r} \cdot \vec{J}) j_l(k_{co}r) \right\} d\vec{r} \tag{B2a}$$

$$a_M(l,m) = -i \cdot k_{co}^2 / \sqrt{l(l+1)} \cdot \int Y_{lm}^* \vec{\nabla} \cdot (\vec{r} \times \vec{J}) j_l(k_{co}r) d\vec{r} \tag{B2b}$$

$Z_{co} = \sqrt{\mu_0 / \varepsilon_{co}}$ is the material impedance and $k_{co} = \sqrt{\varepsilon_{co} / \varepsilon_0}\,\omega_0 / c_0$ is the wave vector. Here ε_{co} is the constant permittivity of the core material. The source current is $\vec{J} = -i\omega_0 p_0 \delta(\vec{r} - \vec{r}_0)\hat{\vec{\alpha}}$ and the charge density is $\rho = -p_0 \vec{\nabla} \delta(\vec{r} - \vec{r}_0)\hat{\vec{\alpha}}$, then Eq. (B2a) and (B2b) can be simplified to

$$a_E(l,m) = k_{co} J_0 / \sqrt{l(l+1)} \cdot \hat{\vec{\alpha}} \cdot \vec{\nabla} \times \vec{\nabla} \times \left[\vec{r} j_l(k_{co}r) Y_{lm}^*(\theta,\varphi) \right] \Big|_{\vec{r}=\vec{r}_0} \tag{B3a}$$

$$a_M(l,m) = i\,k_{co}^2 J_0 / \sqrt{l(l+1)} \cdot \hat{\vec{\alpha}} \cdot \vec{\nabla} \times \left[\vec{r} j_l(k_{co}r) Y_{lm}^*(\theta,\varphi) \right] \Big|_{\vec{r}=\vec{r}_0} \tag{B3b}$$

where $J_0 = -i\omega_0 p_0$ is again the dipole current amplitude. The total field inside the cavity core is composed of the direct radiation field of the dipole (Eq. (B1)) plus the field reflected from the boundary, i.e.

$$\vec{E}_{core} = \vec{E}_{dip} + \vec{E}_{ref} \tag{B4}$$

The reflected field is source-free and can be expanded as

$$\vec{E}_{ref} = Z_{co} \sum_{l,m} \left[i/k_{co} \cdot b_E(l,m)\vec{\nabla} \times j_l(k_{co}r)\vec{X}_{lm} + b_M(l,m) j_l(k_{co}r)\vec{X}_{lm} \right] \tag{B5}$$

The total radiation field outside the Bragg sphere is

$$\vec{E}_{rad} = Z_{out} \sum_{l,m} \left[i/k_{out} \cdot c_E(l,m)\vec{\nabla} \times h_l^1(k_{out}r)\vec{X}_{lm} + c_M(l,m)h_l^1(k_{out}r)\vec{X}_{lm} \right] \tag{B6}$$

where $Z_{out} = \sqrt{\mu_0 / \varepsilon_{out}}$, $k_{out} = \sqrt{\varepsilon_{out} / \varepsilon_0}\,\omega_0 / c_0$ and ε_{out} is the constant permittivity of the material outside the Bragg sphere. Since the fields inside the core and that outside the sphere are related to each other by the boundary condition, we can use the transfer matrix method

#71220 - $15.00 USD Received 25 May 2006; revised 19 July 2006; accepted 20 July 2006

described in section II again. With Eq. (B4)-Eq. (B6), the coefficients in the transfer matrix Eq. (10) are found to be

$$\begin{aligned} A_{co}^{l} &= a_E(l) + b_E(l)/2,\ B_{co}^{l} = b_E(l)/2,\ A_{out}^{l} = c_E(l),\ B_{out}^{l} = 0 \\ C_{co}^{l} &= a_M(l) + b_M(l)/2,\ D_{co}^{l} = b_M(l)/2,\ C_{out}^{l} = c_M(l),\ D_{out}^{l} = 0 \end{aligned} \tag{B7}$$

and Eq. (10) leads to

$$c_E = a_E \Big/ \left[\left(M_l^{TM}\right)_{1,1} - \left(M_l^{TM}\right)_{2,1} \right] \ \&\ \ b_M = a_M \Big/ \left[\left(M_l^{TE}\right)_{1,1} - \left(M_l^{TE}\right)_{2,1} \right] \tag{B8}$$

The total radiation power is an incoherent sum of the contributions from all the multipole modes [28]

$$P_{cav} = Z_{out} \Big/ \left(2k_{out}^2\right) \cdot \sum_{l,m} \left[\left|c_E(l,m)\right|^2 + \left|c_M(l,m)\right|^2 \right] \tag{B9}$$

and the radiation power of an oscillating dipole in the bulk core material is $P_{bulk} = \sqrt{\varepsilon_{co}/\varepsilon_0} \cdot \omega_0^4 / \left(12\pi\varepsilon_0 c_0^3\right) \cdot \left|p_0\right|^2$ [3]. Substituting Eq. (B3a)-(B3b) and Eq. (B8) into Eq. (B9), the normalized decaying rate is

$$\frac{b}{b_0} = \frac{P_{cav}}{P_{bulk}} = \left(\frac{\varepsilon_{co}}{\varepsilon_{out}}\right)^{3/2} 12\pi \sum_{lm} \frac{1}{2} \left| \frac{1}{\left(M_l^{TM,TE}\right)_{1,1} - \left(M_{2,1}^{TM,TE}\right)_{2.1}} \right|^2 \left| \vec{\alpha} \cdot \vec{E}_{lm}^{TM,TE}\left(k_{co}\vec{r}_0\right) \right|^2 \tag{B10}$$

where the vectors $\vec{E}_{lm}^{TM,TE}$ are defined in Eq. (A8a)-(A8b) and the superscript *TM,TE* means summation over both TM and TE modes.

In the following we are going to prove Eq. (B10) is equivalent to Eq. (13a). For a pure multipole mode of order (*l*,*m*) described by Eq. (8a)-(8b), by integrating the poynting vector over all solid angle, we obtain the radiation power in the *n*th layer [28]

$$P = Z_n \big/ 2k_n{}^2 \cdot \left(\left|A_n\right|^2 - \left|B_n\right|^2 \right) \ \text{(TM mode)} \ \&\ \ P = Z_n \big/ 2k_n{}^2 \cdot \left(\left|C_n\right|^2 - \left|D_n\right|^2 \right) \ \text{(TE mode)} \tag{B11}$$

When there is no gain or loss inside the cladding media, the energy flux on the inner and outer sides of the cladding layer should be equal to each other due to the energy conservation law. If the materials in the core and outside the Bragg onion sphere are the same we derive

$$\left(\left|A_{co}\right|^2 - \left|B_{co}\right|^2 \right) = \left(\left|A_{out}\right|^2 - \left|B_{out}\right|^2 \right) \ \&\ \ \left(\left|C_{co}\right|^2 - \left|D_{co}\right|^2 \right) = \left(\left|C_{out}\right|^2 - \left|D_{out}\right|^2 \right) \tag{B12}$$

Combine above results with Eq. (10) and use the boundary condition that there is no incident wave from outside, i.e. $B_{out} = 0$ and $D_{out} = 0$, we can prove

$$\left|\left(M_l\right)_{1,1}\right|^2 - \left|\left(M_l\right)_{2,1}\right|^2 = 1 \tag{B13a}$$

$$1 + 2\,\mathrm{Re}\left(\frac{\left(M_l\right)_{2,1}}{\left(M_l\right)_{1,1} - \left(M_l\right)_{2,1}} \right) = \left| \frac{1}{\left(M_l\right)_{1,1} - \left(M_l\right)_{2,1}} \right|^2 \tag{B13b}$$

for both TE and TM modes. In addition, we notice that without the presence of the cavity, Eq. (B1) and Eq (B6) describe the same radiation field, i.e. $c_E = a_E$ and $c_M = a_M$, then Eq (B10) leads to

$$12\pi \sum_{lm} \left| \vec{\alpha} \cdot \vec{E}_{lm}^{TM,TE}\left(k_{co}\vec{r}_0\right) \right|^2 / 2 = 1 \tag{B14}$$

#71220 - $15.00 USD Received 25 May 2006; revised 19 July 2006; accepted 20 July 2006

Finally, by substituting Eq. (B13b) and Eq. (B14) into Eq. (B10) we immediately find

$$\frac{b}{b_0} = \frac{P_{cav}}{P_{bulk}} = 1 + 12\pi \sum_{lm} \mathrm{Re}\left(\frac{\left(M_l\right)_{2,1}^{TM,TE}}{\left(M_l\right)_{1,1}^{TM,TE} - \left(M_l\right)_{2,1}^{TM,TE}} \right) \cdot \left| \vec{\alpha} \cdot \vec{E}_{lm}^{TM,TE}\left(k_{co}\vec{r}_0\right) \right|^2 \qquad \text{(B15)}$$

which is the same as Eq. (13a).

#71220 - $15.00 USD Received 25 May 2006; revised 19 July 2006; accepted 20 July 2006